UC Berkeley
Precision Manufacturing Group

Title
Copper CMP Modeling: Millisecond Scale Adsorption Kinetics of BTA in Glycine-Containing Solutions at pH 4

Permalink
https://escholarship.org/uc/item/0pn4r425

Authors
Choi, Seungchoun
Tripathi, Shantanu
Dornfeld, David
et al.

Publication Date
2010-10-28

Peer reviewed

eScholarship.org Powered by the California Digital Library
University of California

Journal of The Electrochemical Society, **157** (12) H1153-H1159 (2010)
0013-4651/2010/157(12)/H1153/7/$28.00 © The Electrochemical Society

Copper CMP Modeling: Millisecond Scale Adsorption Kinetics of BTA in Glycine-Containing Solutions at *p*H 4

Seungchoun Choi,[a] Shantanu Tripathi,[a] David A. Dornfeld,[a] and Fiona M. Doyle[b,*,z]

[a]*Department of Mechanical Engineering and* [b]*Department of Materials Science and Engineering, University of California, Berkeley, Berkeley, California 94720, USA*

Millisecond scale benzotriazole (BTA) adsorption kinetics in acidic aqueous solution containing 0.01 M glycine and 0.01 M BTA have been investigated. Chronoamperometry was used to measure current densities on the surface of a micro-copper electrode in *p*H 4 aqueous solutions containing 0.01 M glycine with or without 0.01 M BTA. In the presence of BTA the current density decreased as the inverse of the square root of time for a few seconds due to adsorption of BTA. At potentials above 0.4 V saturated calomel electrode the current leveled off after a second or so due to the formation of a Cu(I)BTA monolayer on the copper surface. Based on these data a governing equation was constructed and solved to determine the initial kinetics of BTA adsorption. Analysis shows that material removal during copper chemical mechanical planarization (CMP) in this slurry chemistry occurs mostly by direct dissolution of copper species into the aqueous solution rather than mechanical removal of oxidized or pure copper species and that each interaction between a pad asperity and a given site on the copper removes only a small fraction of the Cu(I)BTA species present at that site.
© 2010 The Electrochemical Society. [DOI: 10.1149/1.3499217] All rights reserved.

Manuscript submitted June 14, 2010; revised manuscript received September 17, 2010. Published October 28, 2010.

Chemical mechanical planarization (CMP) is used widely for local and global planarization of wafers in the manufacture of integrated circuits. Copper is the metal of choice for interconnects because of its high conductivity and high resistance to electromigration. Copper interconnects are fabricated using the dual damascene process, in which CMP plays a crucial role for removing excess copper and planarizing damascene structures. As the semiconductor industry ramps to 32 nm feature size,[1] there is an increasing need for a robust copper CMP model for successful implementation of design for manufacturability. Although Preston's equation[2] has been widely accepted for wafer-scale CMP modeling, its treatment of CMP as an exclusively mechanical process is overly simplistic. Hence it has limited applicability to CMP processes where chemical or electrochemical mechanisms are known to be at play, such as copper CMP. This limitation has been an impetus for developing many CMP models[3-8]but despite various degrees of success, most of these models fail to fully capture the synergy between mechanical and chemical phenomena.

Recently, Tripathi et al. recognized this synergy in their mechanistic tribochemical model of copper CMP.[9] They argued that during copper CMP, material is primarily removed by wear-induced corrosion. Under typical CMP conditions, where the slurry chemistry allows inhibitor layers or passive films to form on copper, the oxidation rate of copper decreases as the protective surface films progressively grow. At a given site on the copper there will be periodic removal of the protective film during polishing (for example by interaction with abrasive particles and pad asperities), causing a sudden increase in oxidation rate, followed by formation and progressive growth of new passive film, with a concurrent decrease in oxidation kinetics. Copper oxidizes throughout the intervals between these interactions. Some of the oxidized copper forms the passive film and is subsequently removed mechanically and some dissolves directly into solution, but both processes contribute to the removal of copper. The amount of protective film generated between successive asperity–pad interactions and then removed will depend on the interval between the interactions, determined by the pad geometry and rotational velocity relative to the wafer; the chemical conditions, which determine the passivation kinetics; and the amount of passive film remaining after the preceding asperity–copper interaction, which depends on how the protective film interacts (both mechanically and chemically) with abrasive particles and/or pad asperities. The total amount of copper removed at a specific point is given by the cumulative amount of protective film removed plus all direct dissolution from the copper (which is influenced by the amount of remaining protective material on copper surface). Since it is difficult to characterize the transient surface condition of copper at every asperity or abrasive contact during CMP (i.e., how thick the film is or what fraction of reactive surface sites are covered by protective species), Tripathi et al. postulated a quasisteady state for a more computationally efficient numerical implementation of the model.[9] The details of this are discussed below. To explore the model, the passivation kinetics of copper in both acidic and alkaline slurries were studied by potential-step chronoamperometry with a copper microelectrode, using electrochemical impedance spectroscopy (EIS) data to distinguish capacitive charging from faradaic currents.[10]

However, as noted above, the current density measured during potential-step chronoamperometry measures the total rate of copper oxidation. To numerically implement the CMP model, one needs to know the portion of the overall current density attributable to direct dissolution and the portion due to the formation of the protective film. Here we analyze the current densities measured during potential-step chronopotentiometry in an acidic (*p*H 4) solution containing benzotriazole (BTA) as a corrosion inhibitor and glycine as a complexing agent for copper. We deduce the millisecond scale kinetics of adsorption of BTA onto copper surfaces, the current due to the formation of the protective BTA layer, the current due to direct dissolution, and the fractional coverage of copper by BTA during typical CMP operations. This gives significant insight into the molecular scale mechanism of copper CMP in acidic slurries containing inhibitors.

Chronoamperometry Experiments

Using potential-step chronoamperometry, we have measured the current decay of a bare copper microelectrode exposed to two different aqueous solutions buffered at *p*H 4 using acetic acid/sodium acetate, containing either 0.01 M glycine, which complexes copper ions, or 0.01 M glycine and 0.01 M BTA. Full details of the experimental setup and procedures are provided elsewhere,[10] but in brief, a copper microelectrode was conditioned at a cathodic potential between −1.5 and −1 V for 30 s to reductively remove any oxidized surface films, and then stepped up to an oxidizing potential, recording the current as a function of time over short time periods relevant to the intervals between the interaction of pad asperities with the wafer surface in copper CMP. All potentials are reported with respect to the saturated calomel electrode (SCE), unless otherwise stated. Figure 1 shows the current measured experimentally after stepping up to different potentials from −1.2 V (SCE) in *p*H 4 aque-

* Electrochemical Society Active Member.
[z] E-mail: fmdoyle@berkeley.edu

Downloaded 19 Jan 2011 to 128.32.164.247. Redistribution subject to ECS license or copyright; see http://www.ecsdl.org/terms_use.jsp

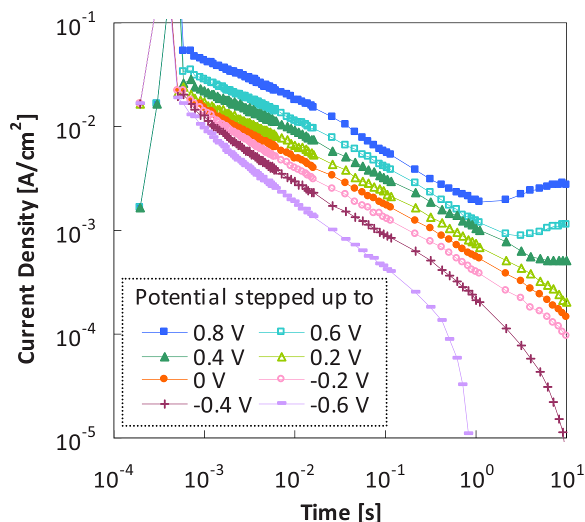

Figure 1. (Color online) Current decay after stepping up from −1.2 V to different potentials, copper in *p*H 4 aqueous solution containing 0.01 M glycine and 0.01 M BTA.

ous solution containing both 0.01 M glycine and 0.01 M BTA. The current decay is very similar for all potentials. EIS data for these conditions, reported elsewhere,[11] predict that capacitive charging should be over in less than a millisecond, since the maximum $R_U C_{DL}$ is 0.3 ms. After this time, Fig. 1 shows that at most final potentials, the current decays at a remarkably constant and similar rate of 0.5 orders of magnitude per decade of time; that is, the current density varies as the inverse of the square root of time. The behavior is very different in the absence of BTA (Fig. 2). At first sight this suggests a Cottrell-type decay behavior in the presence of BTA (Fig. 1), with current densities determined by diffusion of BTA to the copper surface. However, given the fact that the current is strongly affected by the fraction of sites occupied by BTA, as discussed below, there is no compelling evidence for diffusion control. At lower potentials (< -0.2 V) in Fig. 1, the anodic currents eventually became lower in magnitude than the cathodic current due to hydrogen evolution, causing the net current to become cathodic.

Several researchers have examined the interaction of BTA with copper substrates, both adsorption[12-14] and the formation of polymeric CuBTA films,[15-19] albeit over much longer time scales than those studied here. A 1:1 stoichiometric association of Cu with BTA^- in adsorbed layers indicates the formation of a Cu(I) species.[19-24] BTA has been reported to adsorb on copper at low *p*H, lower potentials, and low adsorption densities, while polymerized Cu(I)BTA multilayers appear at high *p*H, higher potentials, and higher adsorption densities.[14,20,25-31] Adsorption has been reported on both oxide-free copper surfaces and Cu_2O.[21,32-35] Youda et al.[25] and Tromans[26,36] presented Eh–*p*H diagrams that show Cu(I)BTA predominating at *p*H 4 aqueous solutions at oxidizing potentials, but these are equilibrium diagrams and may not reflect the dynamic condition during active polishing of copper, where any adsorbed BTA is regularly disturbed by pad asperities and copper is continuously oxidized. Nevertheless, it is evident that the copper on the surface is oxidized to form a protective layer of BTA.

At some of the higher potentials in Fig. 1 (> 0.4 V), the current densities leveled off after a few seconds. This suggests that either there is no more adsorption of BTA or any subsequent adsorption of BTA provides no further passivity. Although at first sight the transition could be associated with a change in behavior for either a monolayer or a Cu(I)BTA multilayer, it is unlikely that a multilayer could have developed to the point of establishing a limiting current in just a few seconds. Furthermore, since the formation of a monolayer involves diffusion of BTA through the boundary layer at the copper–solution interface whereas the formation of a Cu(I)BTA multilayer involves transport of species through layers that had already formed, which is much slower than boundary layer diffusion, one would expect a change in gradient when monolayer formation changed to multilayer formation. As discussed above, the change in gradient in Fig. 1 below 1 ms has been correlated with the cessation of capacitive charging, and there are no further changes in gradient until those seen at a few seconds. Hence, this point can reasonably be assumed to correspond to complete occupation by BTA of all available anodic sites on the copper surface, i.e., the formation of a protective monolayer on the copper surface. The time at which the monolayer first forms is designated as t_m. Any subsequent uptake of BTA is assumed to correspond to the precipitation of polymerized multilayers by the interaction of copper ions that had previously dissolved into the aqueous solution with BTA species diffusing to the surface region from the bulk. If this is the case, the removal of the precipitated layers would not contribute to the material removal during copper CMP, regardless of the amount of copper within them, because this copper will have already have been accounted for as direct dissolution from the copper surface.

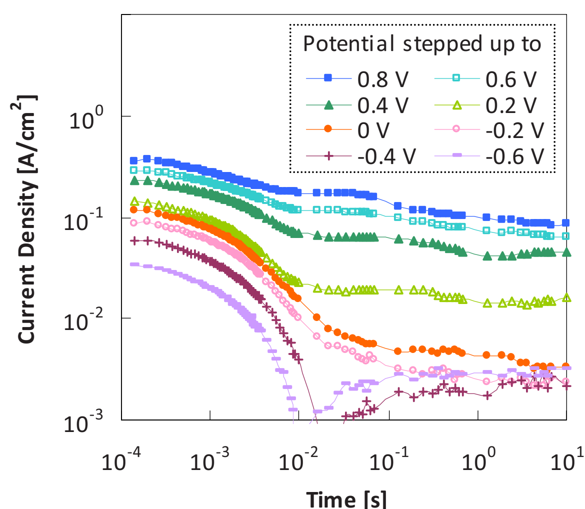

Figure 2. (Color online) Current decay after stepping up to different potentials from −0.9 V (using fixed range data acquisition), copper in *p*H 4 aqueous solution containing 0.01 M glycine.

Quasisteady-State Assumption

As noted above, for computational efficiency Tripathi et al. postulated a quasisteady state during copper CMP such that on average the amount of protective film removed at each asperity–copper interaction is equal to the amount of film that reforms before the next interaction.[9] In principle, the estimation could have considered successive abrasive particle–copper interactions rather than asperity–copper interactions. However, the interval between sequential abrasive particle–copper interactions under an asperity was estimated at less than 10 μs, which is 2 or 3 orders of magnitude smaller than the interval between asperity–copper interactions (1–10 ms).[9] Hence the electrochemical changes on copper between sequential abrasive contacts under the same asperity would be minor compared to the electrochemical changes occurring between two asperity contacts. Indeed, assuming that the abrasive particles are relatively uniformly distributed under each asperity, they can be considered part of the asperity itself and most likely provide the "chemical tooth"[3] that preferentially interacts with Cu–BTA complexes. Therefore, only the interval between two consecutive asperity–copper interactions was considered in the concept of a quasisteady state.

The oxidation rates shown in Fig. 1 decrease from about 0.05 A/cm^2 immediately after capacitive charging has ceased to about 0.003 A/cm^2 or less at t_m, equivalent to material removal rates declining from about 1100 to 66 nm/min or less (assuming that

Downloaded 19 Jan 2011 to 128.32.164.247. Redistribution subject to ECS license or copyright; see http://www.ecsdl.org/terms_use.jsp

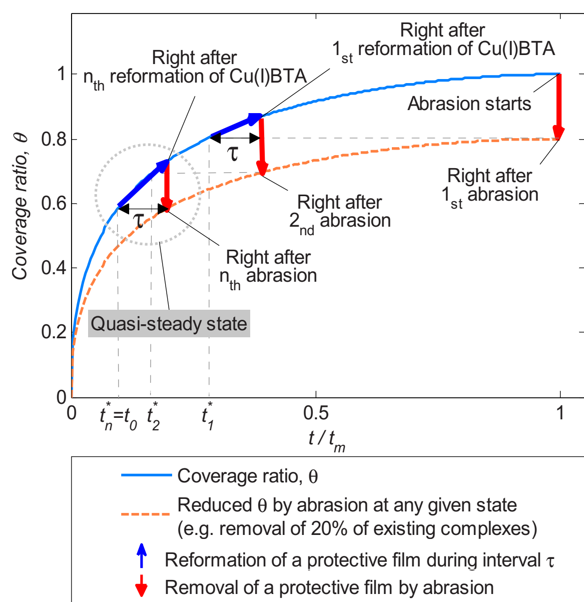

Figure 3. (Color online) Establishment of the quasisteady state when there is less than a monolayer of protective material on the copper surface.

Cu(II) is formed). For copper CMP in slurries containing BTA and glycine, typical material removal rates are 130–600 nm/min.[37] Since these rates lie between the rates corresponding to the extreme currents seen in Fig. 1, it appears that during most copper CMP operations there is less than a monolayer of BTA on the copper.

Figure 3 schematically illustrates the establishment of the quasisteady state when the copper surface is partially covered by Cu(I)BTA between pad asperity–copper interactions. The upper curve shows the fraction of the copper surface sites occupied by Cu(I)BTA at any time. It is assumed that an asperity moving across the surface will remove a constant fraction of all the Cu(I)BTA present. [It is implicit in this assumption that the mechanism for removing Cu(I)BTA species is preferential adsorption onto abrasive particles held under the asperity and that the abrasive particles themselves will already have some sites occupied by Cu(I)BTA because of either previous interactions with copper or through having adsorbed dissolved copper and BTA in the slurry.] Figure 3 was constructed assuming (arbitrarily, to illustrate the principle involved) that 20% of the Cu(I)BTA species present on the copper surface at any time are removed by a given interaction with a pad asperity regardless of the absolute concentration of the species on the surface (shown as the dashed line). It is assumed that when abrasion starts there is a monolayer of Cu(I)BTA present (at least a monolayer is reasonable, given that the time taken to move a copper-covered wafer into position above a polishing pad exceeds the values for t_m seen in Fig. 1] and that the fraction of surface sites occupied by Cu(I)BTA after the first interaction corresponds to the state at t_1^* (indicated by the downward arrow and horizontal dashed line). More Cu(I)BTA forms on the copper surface before the next asperity–copper interaction (indicated by the upward arrow) but the time, τ, until the next interaction is not long enough to reform a monolayer. Accordingly, the next abrasion [again assuming that it removes 20% of all Cu(I)BTA on the surface] will further reduce the coverage of the surface by Cu(I)BTA beyond that achieved in the first interaction to one corresponding to a different state at t_2^*. This process is repeated n times until a quasisteady state is reached where exactly as much Cu(I)BTA is removed during an asperity–copper interaction as is reformed in the interval before the next interaction, τ (at t_n^*). Note that the duration of the asperity–copper interaction is very short compared to the interval between asperity–copper contacts and no significant electrochemical reaction occurs during the interaction itself. (The electrochemical state at the beginning of a single interaction is almost the same as that at the end of the interaction.) Hence the asperity–copper interactions are denoted by vertical lines, while the reformation of Cu(I)BTA is relatively gradual and is shown as diagonal lines.

Although Fig. 3 was constructed for an initial condition of monolayer coverage of copper by Cu(I)BTA, the same principles would be applicable to an initial state with thicker polymeric Cu(I)BTA multilayers. Conversely, if there is bare copper when abrasion starts (less likely), a quasisteady state is eventually reached because of net growth of the protective layer resulting from repetitive abrasion and BTA adsorption.

Regardless of the initial condition, because the reduction of coverage upon abrasion and the gain in the coverage during τ is always equal once the quasisteady state has been reached, the vertical and diagonal arrows in Fig. 3 cycle inside of the dashed circle [i.e., the fractional coverage immediately after the nth abrasion is the same as that immediately after the $(n + 1)$th abrasion]. This introduces the time parameter t_0, defined by

$$t_n^* = t_{n+1}^* = t_{n+2}^* = \cdots \equiv t_0 \quad [1]$$

Faraday's law can be invoked to express the balance between the amount of Cu(I)BTA formed at the surface and the amount removed

$$\int_{t_0}^{t_0+\tau} i_{pass}(t)dt = \Delta q(t_0 + \tau) \quad [2]$$

where $\Delta q(t)$ is the charge density of the oxidized copper within the Cu(I)BTA removed from the copper surface during an abrasion event at time t, $i_{pass}(t)$ is the current density that contributes to the formation of Cu(I)BTA on the surface at time t, and τ is the interval between abrasion events when a quasisteady state is reached.

The material removal rate (MRR) (which becomes constant once the quasisteady state has been reached) is given by

$$\text{MRR} = \frac{M_{\text{Cu}}}{\rho n F \tau}\int_{t_0}^{t_0+\tau} i_{total}(t)dt \quad [3]$$

where i_{total} is the total oxidation rate, including both the current density responsible for forming the first layer of Cu(I)BTA on the surface (i_{pass}) and the current density responsible for direct dissolution of copper ions into the solution (i_{diss}) (which will eventually form soluble copper complexes with glycine[38,39] or the acetate buffer or as mentioned above, may reprecipitate with BTA). M_{Cu} is the atomic mass of copper, ρ is the density of copper, n is the oxidation state of the oxidized copper, and F is Faraday's constant. However, before the integral in Eq. 3 can be evaluated using the kinetics of current decay shown in Fig. 1, it is necessary to determine where t_o lies.

Theoretical Analysis

Given that the intervals between two asperity–copper contacts for typical operating parameters during CMP are around 1–10 ms,[9] the thickness of copper that is removed between each interaction (due to both dissolution between the two interactions and removal of oxidized copper film by the interaction) is equivalent to about 0.1–1 Å. This is less than the atomic radius of copper, 1.4 Å. Because it is clearly impossible to remove a fraction of a copper atom, this low average means that the likelihood that a given surface copper species is removed in any given interaction is well below unity. The "mechanical" phenomena during copper CMP, which have hitherto been envisaged as mechanical damage to a passive film (as first proposed by Kaufman[8]), are evidently more akin to the plucking of certain atoms or molecules from an incompletely covered surface during each abrasive interaction. This appears completely consistent with Cook's "chemical tooth" model[3] but suggests far less mechanical action in CMP than is considered in most models.

The small amount of material removed with each asperity–copper interaction, in conjunction with the establishment of a qua-

Downloaded 19 Jan 2011 to 128.32.164.247. Redistribution subject to ECS license or copyright; see http://www.ecsdl.org/terms_use.jsp

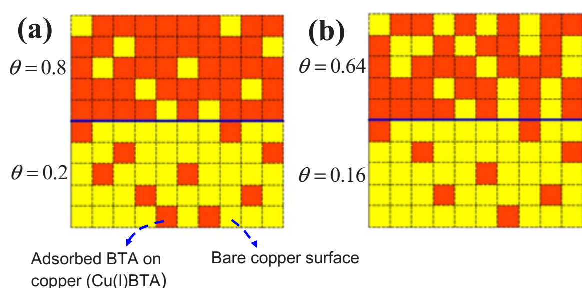

Figure 4. (Color online) Coverage ratio change (a) before and (b) after asperity contact during copper CMP. The removal efficiency η is assumed to be 0.2.

sisteady state in the sub-monolayer regime, implies that Cu(I)BTA only covers a fraction of the copper surface between asperity–copper interactions and each interaction only removes a portion of this oxidized material. This situation is illustrated schematically in Fig. 4. Figure 4a shows the surface condition right before abrasion (i.e., at $t_0 + \tau$), and Fig. 4b shows the surface immediately after an abrasion event that removed 20% of the total adsorbed Cu(I)BTA (i.e., at t_0). It is assumed that the Cu(I)BTA species are randomly distributed on the surface and that abrasion will remove a constant fraction of the total number of Cu(I)BTA species present on the surface. The arbitrary percentage chosen (20%) was selected for consistency with Fig. 3. The removal efficiency, η, can be expressed as

$$\Delta q = \eta q \quad (0 \leqslant \eta \leqslant 1) \qquad [4]$$

where q is the charge density of the oxidized copper that constitutes the Cu(I)BTA on the copper surface before abrasion.

To the best of our knowledge the kinetics for forming a monolayer of protective film in a pH 4 aqueous solution containing glycine and BTA have not been studied to date, and it would be challenging to investigate the kinetics in this regime by direct experimental measurement. The electrochemical quartz crystal microbalance (EQCM) technique has been employed to study the kinetics of forming multilayers of BTA over time scales of the order of hours.[40,41] Unfortunately, the resolvable time scale of the EQCM, about 0.1 s,[42] limits the usefulness of this technique for studying the millisecond time scale. Hence, we employed a theoretical approach using our experimental chronoamperometric data to determine the rates of dissolution of copper from bare copper sites and from the sites that are occupied by BTA and then used these data to calculate the kinetics of adsorption of BTA onto copper.

The experimentally measured current densities in Figs. 1 and 2 include current that leads to the formation of the protective film and current that leads to direct dissolution of the copper. As noted above, the total current was inversely proportional to the square root of time

$$i_{total} = i_{pass} + i_{diss} = i_m\left(\frac{t}{t_m}\right)^{-0.5} \quad \text{for } t \leqslant t_m \qquad [5]$$

where i_m is the current density at t_m.

The current density responsible for forming adsorbed Cu(I)BTA can be written as

$$i_{pass}(t) = \frac{dq}{dt} = c\frac{d\theta}{dt} \qquad [6]$$

where θ is the fractional coverage and c is a constant that relates the fractional coverage to the charge density of the oxidized copper that constitutes the Cu(I)BTA on the copper surface.

The constant c is easily evaluated. When a complete Cu(I)BTA monolayer has formed (i.e., θ = 1), q is equal to c (by $q = c\theta$). Hence c is given by

$$c = neN \qquad [7]$$

where n is unity for Cu(I), e is the elementary charge, 1.602176 $\times 10^{-19}$ C/electron, and N is the surface density of Cu(I)BTA on the surface.

Assuming that copper dissolves directly into the solution from both bare sites and those on which BTA is adsorbed but with different potential-dependent rate constants denoted by a and b, respectively, and that these rate constants are independent of the fractional coverage, θ, the current density, for the direct dissolution of copper can be written as

$$i_{diss} = a(1-\theta) + b\theta \qquad [8]$$

Combining Eqs. 5, 6, and 8 gives the following linear differential equation that governs the kinetics of BTA adsorption for $t \leqslant t_m$

$$a(1-\theta) + b\theta + c\frac{d\theta}{dt} = i_m\left(\frac{t}{t_m}\right)^{-0.5} \quad \text{or}$$

$$\frac{d\theta}{dt} = \frac{i_m}{c}\left(\frac{t}{t_m}\right)^{-0.5} + \frac{a-b}{c}\theta - \frac{a}{c} \qquad [9]$$

Solving the first order differential equation using the boundary condition $\theta_{t=0} = 0$ yields

$$\theta(t) = \left[\frac{i_m\sqrt{t_m}\sqrt{\pi}}{\sqrt{c(a-b)}}\operatorname{erf}\left(\sqrt{\frac{a-b}{c}t}\right) + \frac{a}{a-b}e^{-\left(\frac{a-b}{c}t\right)} - \frac{a}{a-b}\right]e^{\frac{a-b}{c}t} \qquad [10]$$

From Eq. 9 and the definition of t_m, it is apparent that at t_m, θ = 1 and $d\theta/dt = 0$, hence

$$b = i_m \qquad [11]$$

This is consistent with the oxidation rate at t_m being exclusively due to the dissolution of copper from BTA adsorbed sites. The coefficient a can be determined from the oxidation rate at t_m in a solution that does not contain BTA, which is given by Fig. 2. The coefficient c can be calculated from Eq. 10 using the determined coefficients a and b and the condition at t_m (θ = 1). The adsorption density of BTA at monolayer coverage can then be determined from Eq. 7 and the kinetics of adsorption evaluated from Eq. 10.

For pH 4 aqueous solution containing glycine and BTA, one can use material removal rates reported in the literature to estimate the position of quasisteady state under typical conditions, assuming that the kinetics of BTA adsorption would be similar under polishing conditions to those for the microelectrode. Substituting Eqs. 5 and 11 into Eq. 3 gives

$$MRR = \frac{M_{Cu}}{\rho nF\tau}\int_{t_0}^{t_0+\tau} b\left(\frac{t}{t_m}\right)^{-0.5} dt \qquad [12]$$

$$= \frac{M_{Cu} b\sqrt{t_m}}{\rho nF\tau}\int_{t_0}^{t_0+\tau} \frac{1}{t^{0.5}}dt \qquad [13]$$

$$= \frac{2M_{Cu} b\sqrt{t_m}}{\rho nF\tau}[(t_0+\tau)^{0.5} - t_0^{0.5}] \qquad [14]$$

Thus, knowing the parameters b and t_m for given conditions, one can determine the characteristic time t_o corresponding to the beginning of quasisteady state for a given MRR and value of τ.

Results and Discussion

The kinetics of adsorption of BTA onto a copper microelectrode at 0.6 and 0.4 V (SCE) in a pH 4 aqueous solution containing 0.01 M glycine and 0.01 M BTA (the second and third highest lines in Fig. 1) were modeled using the equations derived. The evaluated coefficients and constants are listed in Table I. Note that the ratio of coefficients a and b (a/b) and the coefficient c are similar at both

Downloaded 19 Jan 2011 to 128.32.164.247. Redistribution subject to ECS license or copyright; see http://www.ecsdl.org/terms_use.jsp

Table I. Derived values for a governing equation of the kinetics of BTA adsorption in a pH 4 aqueous solution containing 0.01 M glycine and 0.01 M BTA.

Potential [V (SCE)]	t_m (s)	a (A/cm^2)	b (A/cm^2)	c (C/cm^2)
0.6	2	7.0×10^{-2}	8.4×10^{-4}	6.26×10^{-5}
0.4	4	4.4×10^{-2}	4.7×10^{-4}	6.24×10^{-5}

potentials, which is physically reasonable. The current density at unoccupied sites (coefficient a) is nearly 2 orders of magnitude higher than that at sites occupied by BTA (coefficient b), which demonstrates the efficacy of BTA as a corrosion inhibitor.

To further assess the validity of the derived values, the coefficient c was converted into the adsorption density of BTA on copper and compared with values in the literature. An upper limit for the adsorption density of Cu(I)BTA on copper surfaces can be estimated from the surface density of the most closely packed copper surface, namely, the (111) surface, 1.77×10^{15} atoms/cm^2.[43] The surface density can also be estimated from the area that each BTA molecule occupies on the copper surface. Xu et al. used the molecular structure of adsorbed BTA reported by Tomas et al.[44] to estimate that each BTA molecule occupies about 35 Å^2 if adsorbed with its molecular plane parallel to the surface, corresponding to a saturation limit of 2.8×10^{14} molecules/cm^2, and about 12 Å^2 if adsorbed with its molecular plane normal to the surface, corresponding to a saturation limit of 8.4×10^{14} molecules/cm^2.[24] Xu et al. also reported the surface density of a monolayer of BTA^- on Cu_2O equilibrated with a neutral pH aqueous BTA solution to be 6.3×10^{14} cm^{-2}.[45] Bastidas reported the projected area of a vertically oriented adsorbed BTA molecule to be about 20 Å^2 (the projected area of a rectangle surrounding the molecule) as compared with 38 Å^2 for the horizontal orientation of BTA,[46] corresponding to surface densities of 5.0×10^{14} molecules/cm^2 and 2.6×10^{14} molecules/cm^2, respectively. Thus, the adsorption density of BTA on copper surface is between 2.6×10^{14} and 8.4×10^{14} molecules/cm^2.

The experimentally evaluated coefficient c in Table I corresponds to BTA adsorption densities of 3.91×10^{14} (at 0.6 V) and 3.89×10^{14} molecules/cm^2 (at 0.4 V) on copper, intermediate between the saturation limits for BTA molecular planes parallel to the surface and normal to the surface. This implies either a range of orientations of BTA molecules in a monolayer or that each BTA molecule is adsorbed onto the surface with its molecular plane tilted with respect to the surface normal. This consistency with independently obtained data affirms the validity of the approach adopted here for determining the adsorption behavior of BTA in pH 4 aqueous solution containing BTA and glycine.

The resulting millisecond scale kinetics of adsorption of BTA onto copper surfaces from acidic aqueous solution are shown in Fig. 5, which shows rapid initial adsorption of BTA onto the copper surface. Within 30 ms (at 0.6 V), more than 90% of the copper surface is occupied by adsorbed BTA. The adsorption kinetics of BTA at 0.4 V are very similar to those at 0.6 V when plotted as a function of normalized time (i.e., t/t_m), despite the differences in the coefficients a, b, and c (inset of Fig. 5).

Substituting the coefficients a, b, and c, along with the adsorption kinetics shown in Fig. 5, into Eqs. 5, 8, and 9 yields Fig. 6, which shows the current density responsible for passivation and the current density for direct dissolution of copper as a function of time during the formation of a monolayer of BTA on copper. It is evident that initially the vast majority of the current is due to the formation of the passive layer, albeit at a steadily declining magnitude. (It should also be recognized that this portion of Fig. 6 is extrapolated, since capacitive charging dominated the current observed in the experimental potential-step chronoamperometry experiments.) At around 0.1 ms the current due to direct dissolution of copper becomes comparable to that due to the formation of the passive layer, and by 1 ms the majority of the current is due to direct dissolution of copper.

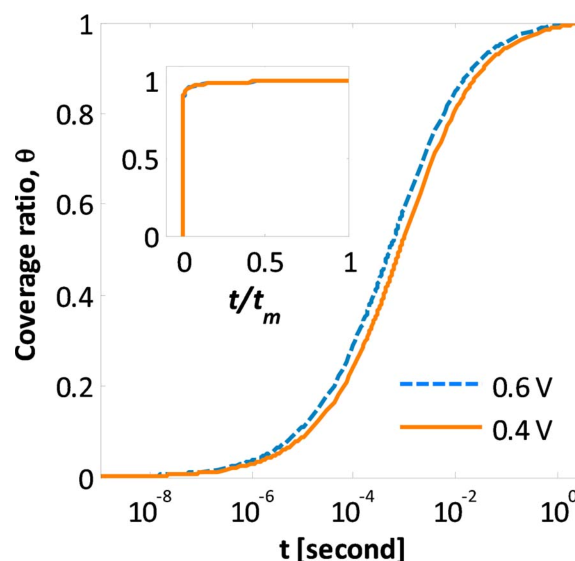

Figure 5. (Color online) Millisecond scale adsorption kinetics of BTA in pH 4 aqueous solution containing 0.01 M glycine and 0.01 M BTA. Inset: Adsorption kinetics over the normalized time in linear scale.

Equation 14 was solved numerically for the different parameters of b and t_m corresponding to potentials of 0.6 and 0.4 V, using the atomic weight of copper (63.54 g/mole) and density (8.96 g/cm^3). The value of n was taken as 2 because although copper is in the +1 oxidation state in adsorbed Cu–BTA complexes, it enters solution in the +2 oxidation state. Two extreme values of material removal rates taken from the literature were considered, namely, 130 and 600 nm/min. Two extreme values of τ were also considered, namely, 1 and 10 ms, values representative of typical pads and rotational velocities. The resulting values of t_o are reported in Table II, along with the values of θ corresponding to these times, and the

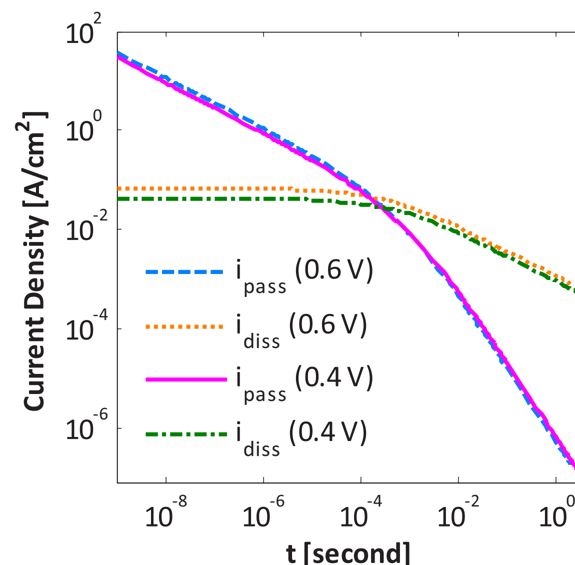

Figure 6. (Color online) Current density for forming Cu(I)BTA and the current density for direct dissolution as a function of time during the formation of a monolayer of BTA on copper.

Downloaded 19 Jan 2011 to 128.32.164.247. Redistribution subject to ECS license or copyright; see http://www.ecsdl.org/terms_use.jsp

Table II. Time corresponding to beginning of quasisteady state, corresponding fractional coverage, and fractional coverage at next asperity–copper interaction, for MRRs and operating conditions typical of copper CMP processes.

Potential [V (SCE)]	t_m (s)	b (A/cm^2)	τ (ms)	MRR (nm/min)	t_o (s)	θ (t_o)	θ ($t_o + \tau$)
0.6	2	8.4×10^{-4}	1	130	4.01068×10^{-2}	0.9273	0.9283
0.6	2	8.4×10^{-4}	10	130	3.57592×10^{-2}	0.9224	0.9326
0.6	2	8.4×10^{-4}	1	600	1.43898×10^{-3}	0.6422	0.7087
0.6	2	8.4×10^{-4}	10	600	N/A	N/A	N/A
0.4	4	4.7×10^{-4}	1	130	2.49268×10^{-2}	0.8777	0.8801
0.4	4	4.7×10^{-4}	10	130	2.06701×10^{-2}	0.8653	0.8902
0.4	4	4.7×10^{-4}	1	600	7.45896×10^{-4}	0.4875	0.6056
0.4	4	4.7×10^{-4}	10	600	N/A	N/A	N/A

values of θ at $t_o + \tau$. There was no physically realistic solution to Eq. 14 for the higher value of τ in conjunction with the higher material removal rate. Physically it is reasonable that high material removal rates would not be seen with slow rotational speeds in CMP. It is seen that for the lowest material removal rates typically encountered in copper CMP, the surface is almost completely covered by BTA throughout the polishing process. The fractional coverage is about 93% at 0.6 V (SCE) and 88% at 0.4 V (SCE), and only a miniscule amount of BTA is removed with each asperity–copper interaction. Under such conditions, essentially all material is removed by direct electrochemical dissolution of copper. Conversely, at the highest material removal rates typically encountered in copper CMP, the copper surface undergoing active polishing is only partially covered by BTA. (Of course recessed areas on the copper surface that do not interact with the pad would be fully protected by thick BTA layers.) Immediately after an asperity–copper interaction, about 64 and 49% of the sites on copper would be occupied by BTA at 0.6 and 0.4 V, respectively. These occupancies would have increased to 71 and 61% after just 1 ms. These conditions correspond to values of t_o of around 1 ms, which from Fig. 6 is the time at which material removal involves both direct dissolution and formation of passive layers. Regardless of the precise material removal rate, it is clear that dissolution is an important material removal mechanism.

Conclusions

The millisecond scale adsorption kinetics of BTA onto copper surfaces in pH 4 aqueous solution containing 0.01 M glycine and 0.01 M BTA have been determined from analysis of potential-step chronoamperometry data. These kinetics show that BTA rapidly adsorbs onto copper surfaces, forming a monolayer of Cu(I)BTA within a second or so. Building on this analysis, we have shown that under typical CMP conditions, with typical material removal rates, copper surfaces undergoing active polishing in acidic slurries containing BTA have less than a monolayer of BTA on the surface. Further, only a small proportion of the adsorbed BTA is removed with any given asperity–copper interaction; most material removal is due to direct dissolution of Cu^{2+} ions (which may subsequently form complexes with other slurry components) into the slurry. This mechanistic picture of copper CMP differs from the commonly accepted model first depicted schematically by Kaufmann et al.[8] for polishing tungsten, involving thick passive layers that are completely removed with each interaction. We have also confirmed that as proposed earlier,[9] CMP in acidic conditions in the presence of BTA is a wear-induced corrosion process rather than a corrosion-enhanced wear process.

Acknowledgments

This work was supported in part by the UC Discovery Grant ele07-10283 under the IMPACT program and AMD, Applied Materials, ASML, Cadence, Canon, Ebara, Hitachi, IBM, Intel, KLA-Tencor, Magma, Marvell, Mentor Graphics, Novellus, Panoramic, SanDisk, Spansion, Synopsys, Tokyo Electron Limited, and Xilinx, with donations from Photronics and Toppan.

The University of California, Berkeley assisted in meeting the publication costs of this article.

References

1. *International Technology Roadmap for Semiconductors (ITRS) 2009 Edition*: http://www.itrs.net/Links/2009ITRS/Home2009.htm.
2. F. W. Preston, *J. Soc. Glass Technol.*, **11**, 247 (1927).
3. L. M. Cook, *J. Non-Cryst. Solids*, **120**, 152 (1990).
4. C. W. Liu, B. T. Dai, W. T. Tseng, and C. F. Yeh, *J. Electrochem. Soc.*, **143**, 716 (1996).
5. S. R. Runnels, *J. Electrochem. Soc.*, **141**, 1900 (1994).
6. F. Zhang and A. Busnaina, *Electrochem. Solid-State Lett.*, **1**, 184 (1998).
7. J. Luo and D. A. Dornfeld, *IEEE Trans. Semicond. Manuf.*, **16**, 45 (2003).
8. F. B. Kaufman, D. B. Thompson, R. E. Broadie, M. A. Jaso, W. L. Guthrie, D. J. Pearson, and M. B. Small, *J. Electrochem. Soc.*, **138**, 3460 (1991).
9. S. Tripathi, S. Choi, F. M. Doyle, and D. A. Dornfeld, *Mater. Res. Soc. Symp. Proc.*, **1157**, E02 (2009).
10. S. Tripathi, F. M. Doyle, and D. A. Dornfeld, *Mater. Res. Soc. Symp. Proc.*, **1157**, E06-02 (2009).
11. S. Tripathi, Ph.D. Thesis, University of California, Berkeley, Berkeley, CA (2008).
12. F. Mansfeld, T. Smith, and E. P. Parry, *Corrosion*, **27**, 289 (1971).
13. G. Lewis, *Br. Corros. J.*, **16**, 169 (1981).
14. D. Thierry and C. Leygraf, *J. Electrochem. Soc.*, **132**, 1009 (1985).
15. N. Morito and W. Suetaka, *J. Jpn. Inst. Met.*, **35**, 1165 (1971).
16. J. J. Kester, T. E. Furtak, and A. J. Bevolo, *J. Electrochem. Soc.*, **129**, 1716 (1982).
17. M. Fleischmann, I. R. Hill, G. Mongoli, and M. M. Musiani, *Electrochim. Acta*, **28**, 1325 (1983).
18. C. Tornkvist, D. Thierry, J. Bergman, B. Liedberg, and C. Leygraf, *J. Electrochem. Soc.*, **136**, 58 (1989).
19. G. W. Poling, *Corros. Sci.*, **10**, 359 (1970).
20. T. Notoya and G. W. Poling, *Corrosion*, **32**, 216 (1976).
21. D. Chadwick and T. Hashemi, *Corros. Sci.*, **18**, 39 (1978).
22. F. El-Taib Heakal and S. Haruyama, *Corros. Sci.*, **20**, 887 (1980).
23. J. Rubim, I. G. R. Gutz, O. Sala, and W. J. Orville-Thomas, *J. Mol. Struct.*, **100**, 571 (1983).
24. Z. Xu, S. Lau, and P. W. Bohn, *Langmuir*, **9**, 993 (1993).
25. R. Youda, H. Nishihara, and K. Aramaki, *Electrochim. Acta*, **35**, 1011 (1990).
26. D. Tromans, *J. Electrochem. Soc.*, **145**, L42 (1998).
27. F. Mansfeld and T. Smith, *Corrosion*, **29**, 105 (1973).
28. M. Metikos-Hukovic, R. Babic, and A. Marinovic, *J. Electrochem. Soc.*, **145**, 4045 (1998).
29. R. Babic, M. Metikos-Hukovic, and M. Loncar, *Electrochim. Acta*, **44**, 2413 (1999).
30. V. Brusic, M. A. Frisch, B. N. Eldridge, F. P. Novak, F. B. Kaufman, B. M. Rush, and G. S. Frankel, *J. Electrochem. Soc.*, **138**, 2253 (1991).
31. M. R. Vogt, W. Polewska, O. M. Magnussen, and R. J. Behm, *J. Electrochem. Soc.*, **144**, L113 (1997).
32. B.-S. Fang, C. G. Olson, and D. W. Lynch, *Surf. Sci.*, **176**, 476 (1986).
33. K. Cho, J. Kishimoto, T. Hashizume, and T. Sakurai, *Jpn. J. Appl. Phys.*, **33**, 125 (1994).
34. S. L. Cohen, V. A. Brusic, F. B. Kaufman, G. S. Frankel, S. Motakef, and B. Rush, *J. Vac. Sci. Technol. A*, **8**, 2417 (1990).
35. J.-O. Nilsson, C. Tornkvist, and B. Liedberg, *Appl. Surf. Sci.*, **37**, 306 (1989).
36. D. Tromans and R. Sun, *J. Electrochem. Soc.*, **138**, 3235 (1991).
37. Q. Luo, S. Ramarajan, and S. V. Babu, *Thin Solid Films*, **335**, 160 (1998).

Downloaded 19 Jan 2011 to 128.32.164.247. Redistribution subject to ECS license or copyright; see http://www.ecsdl.org/terms_use.jsp

38. S. Aksu and F. M. Doyle, *J. Electrochem. Soc.*, **148**, B51 (2001).
39. S. Aksu and F. M. Doyle, *J. Electrochem. Soc.*, **149**, G352 (2002).
40. F. M. Bayoumi, A. M. Abdullah, and B. Attia, *Mater. Corros.*, **59**, 691 (2008).
41. A. Frignani, M. Fonsati, C. Monticelli, and G. Brunoro, *Corros. Sci.*, **41**, 1217 (1999).
42. M. D. Ward and D. A. Buttry, *Science*, **249**, 1000 (1990).
43. M. W. Roberts and C. S. Mckee, *Chemistry of the Metal-Gas Interface*, p. 82, Clarendon, Oxford (1978).
44. F. Tomas, J.-L. M. Abboud, J. Laynez, R. Notario, L. Santos, S. O. Nilsson, J. Catalan, R. Ma. Claramunt, and J. Elguero, *J. Am. Chem. Soc.*, **111**, 7348 (1989).
45. Z. Xu, S. Lau, and P. W. Bohn, *Surf. Sci.*, **296**, 57 (1993).
46. D. M. Bastidas, *Surf. Interface Anal.*, **38**, 1146 (2006).

Downloaded 19 Jan 2011 to 128.32.164.247. Redistribution subject to ECS license or copyright; see http://www.ecsdl.org/terms_use.jsp